buildings

MDPI

Article

Assessment Method for Combined Structural and Energy Retrofitting in Masonry Buildings

Mauro Sassu *, Flavio Stochino and Fausto Mistretta

Department of Civil, Environmental Engineering and Architecture, University of Cagliari, 09123 Cagliari, Italy; fstochino@unica.it (F.S.); fmistret@unica.it (F.M.)
* Correspondence: msassu@unica.it; Tel.: +39-070-675-5409

Received: 29 June 2017; Accepted: 3 August 2017; Published: 11 August 2017

Abstract: The retrofitting of existing masonry buildings is now a crucial problem for Europe. Indeed, structural safety and energy efficiency should represent the target of any renovation. The proposal of a new synthetic performance parameter is presented and discussed. Following this approach, in this paper, after a review of the main studies available in the literature, a proposal of a new performance parameter approach is presented and discussed. It is capable of taking into account both the structural and thermal aspects of masonry retrofitting. An emblematic set of reinforcements and energy improvements for masonry walls is examined. An example, generalized formulas, and a simultaneous evaluation of the role of multiple structural and thermal parameters on masonry buildings are proposed, with a view to optimize several categories of costs related to the intervention.

Keywords: masonry buildings; structural retrofitting; energy retrofitting; combined retrofitting performance; walls refurbishment; generalized performance parameter

1. Introduction

Most of the European traditional buildings are made of masonry. An example of this trend is the graph in Figure 1, representing the impact of masonry constructions built during XX century in Italy. In the past, masonry buildings were often built without structural calculation, only following technical rules or empirical codes. It should be noted that masonry construction has decreased over the years as framed solutions (reinforced concrete (RC) or others) that permit more freedom to the designers have increased. Thus, to assess the structural integrity of such constructions, a thorough review of their current condition has to be perform.

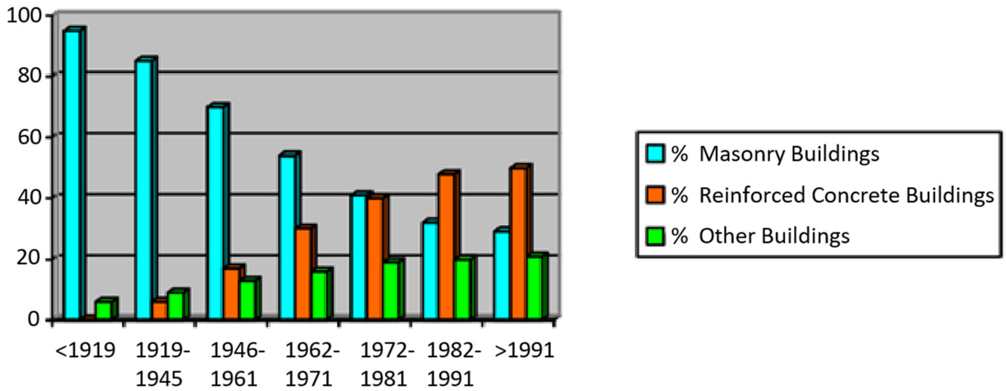

Figure 1. Trend of buildings in Italy during XX century (source ISTAT 2001—Italian Agency of Statistics).

In these cases, to optimize the intervention it is convenient to take into account other aspects, such as thermal and acoustic comfort. Indeed, masonry walls are, at the same time, structural and separating elements.

The CO_2/year emission, joined with the energy spent every year to reach serviceability comfort conditions, represent a primary indicator of the efficiency of the buildings. The most relevant part of energy consumption is commonly represented by the façades. The correct maintenance of their thermal and mechanical properties is crucial: indeed, each construction is subjected to the continuous degradation of structural and energy performance due to environmental actions, anthropic actions, and endogenous ageing (*continuous degradation*). In addition, they can be affected by episodic events like fire [1], explosions [2–4], and seismic actions [5–7] or other phenomena like deliberate attacks or human errors (*discontinuous degradation*). These events can sharply reduce the structural or energy performances of building and their service life. Figure 2 presents a qualitative decrease of performances in the presence of continuous time aging (progressive reduction of performances depending from time) and of traumatic events (discontinuous reduction of performances in case of discrete events). The structural integrity and the energy performance of a building can be described as a monotonic decreasing functions of time with the red lines in Figure 2. After a disruptive event (like fire or impact, earthquake, etc.) there is a sharp transition that modifies these functions and often requires a retrofitting in order to reach the minimum serviceability performance level. In case of an absence of traumatic events, the decay of performances is continuous over time (black lines in Figure 2). After retrofitting, an increase of performance can be achieved (green lines in Figure 2), improving the building condition and lengthening its service life. In this sense it can establish an acceptable level of performances (purple lines in Figure 2) commonly fixed by technical documents, guidelines, or codes.

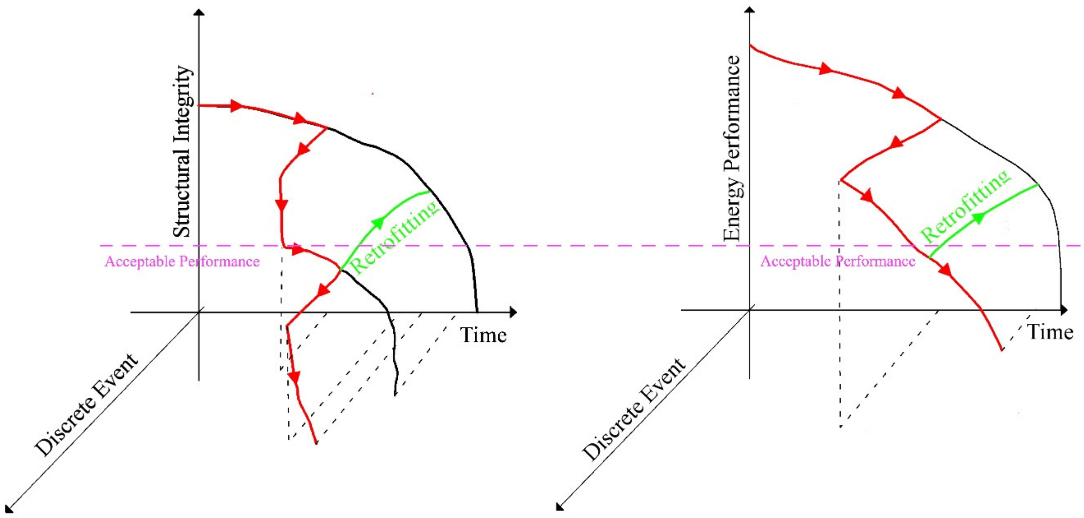

Figure 2. Qualitative evolution of structural and energy performances in the service life of a building.

The opportunity to combine both structural and energy evaluations is relevant to the optimization of resources to address retrofitting strategies. It means the best decision seeks to balance structural and energy improvements. In this sense, structural and energy phenomena are taken into account simultaneously, and the convenience of retrofitting or demolition followed by reconstruction of a building is also assessed.

The cost-benefit analysis, to address an optimum strategy, should be based on a multi-criteria choice: the comfort requirements for a building are of paramount relevance. It should be considered that, in addition, the sustainability awareness of construction life cycles has grown in the last years together with a superior expectation of performance from the buildings. A possible approach could be based on how much energy will be spent for the direct refurbishment and what is the variation of building energy performance.

An example of multi-criteria decision making is in [8], where the main focus is the seismic risk management of existing structures. A recent work of Calvi et al. [9] introduces the idea of a common indicator for both structural and energy performances presenting a cost/benefit analysis for different retrofitting strategies. However, further aspects can be raised in this field. To better explain the strategy here proposed, a flow-chart scheme of the decision phase is drawn in Figure 3. The flow chart describes the several phases of the life of a building. Each of them computes the energy embodied by the building, together with the decision process on refurbishment/demolition-reconstruction choices. If the construction is below the level of "Acceptable Performance" (dashed line of Figure 3) a choice must be made between demolition or refurbishment. Every cost should be considered, and a balance between structural and energy performance should be found.

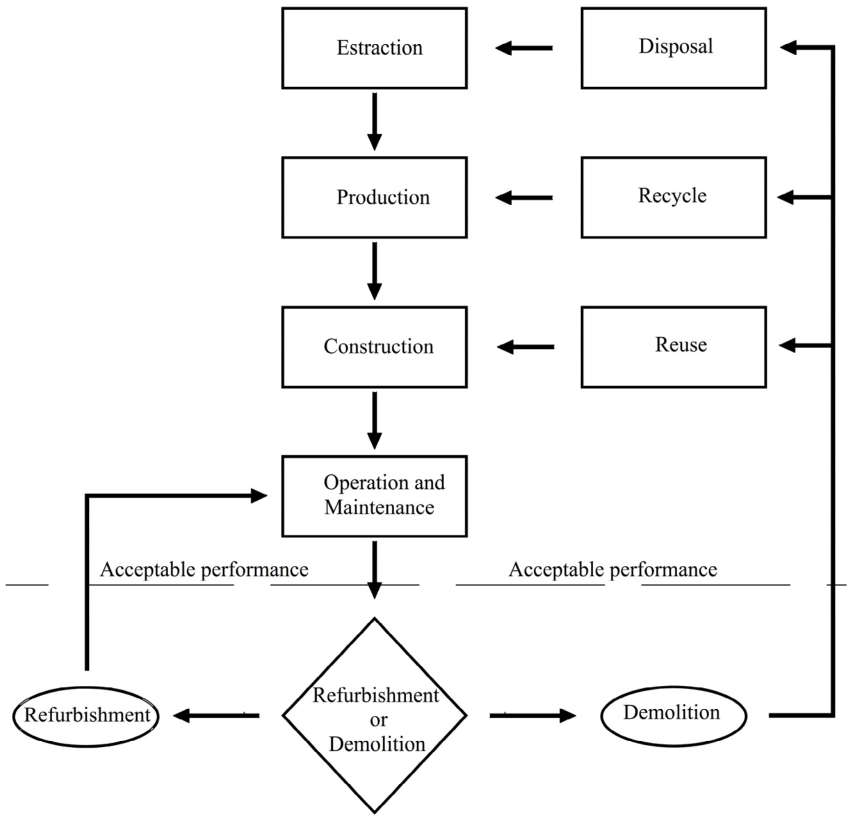

Figure 3. Flow-chart scheme of building assessment decision phase.

After a brief report in Section 2 on the state-of-the-art structural and energy retrofitting techniques for existing masonry constructions, the proposed solution for an integrated approach is discussed in Section 3, based on a simple example of masonry panel. The main idea is to synthesize the decision process throughout a new proposal of dimensionless performance indicators. In Section 4, a generalized approach is presented considering both structural and energy features, proposing a calculation strategy based on the definition of "performance parameter", followed by some conclusive remarks.

2. Retrofitting Techniques

2.1. Structural and Seismic Retrofitting

The problem of structural strengthening in masonry buildings is well known. A synthetic review of the existing methods is reported in [10]. It is possible to group them into surface treatments, grout and epoxy injections, external reinforcements, confining Reinforced Concrete (RC) frames, post tensioning, center core systems. A brief summary of the most used techniques is explained below.

In the set of surface treatments, we consider the old ferrocement system. This consists of multiple layers of reinforcement mesh embedded in a high strength mortar layer [11]. A similar technique is reinforced plaster where high strength steel reinforcements are applied on the wall surface and covered by a thin layer of cement plaster, see [12]. A valid alternative are the shotcrete overalays directly sprayed on the surface of the masonry wall over a mesh of reinforcements, see [13–15]. Textile Reinforced Mortar (TRM) systems denote an inorganic mortar matrix strengthened by an open fabric made of fiber rovings. They have been used to retrofit tuff masonry in [16] and as a strengthening material for generic masonry subjected to in plane and out of plane cyclic loading [17–20]. To restore the original integrity of the retrofitted wall, filling voids and cracks in existing masonry, grout, and epoxy injections represent an efficient tool [21,22].

External reinforcements are common retrofitting techniques; they involve steel plates, tubes, or grids being directly applied to the masonry, thereby improving the lateral in plane resistance of the wall. In [23], externally bonded grids were applied to unreinforced masonry to increase the load-carrying and deformation capacity under cyclic loading. Recent improvements include the *reticulatus* technique [24] which uses a stainless grid which is able to adapt to the irregular texture of blocks. Other traditional techniques, such as the introduction of horizontal steel rods to anchor masonry walls from out-of-plane displacements, can offer relevant improvement against rocking mechanisms [25,26].

The insertion of confining RC frames inside masonry walls allows for the improvement in the energy dissipation capacity and the ductility of the structure, as in [27,28]. This approach is not applicable in most of existing buildings with historical value as it has a wide impact on the structure. Post tensioning denotes the application of a compressive force to the masonry wall which counteracts the tensile stresses produced by the external load, see [29,30]. The cost of this technique and the technological difficulties are often high, so it is generally restricted to monumental buildings. Center core systems denote a grouted reinforced core inserted in the center of an existing masonry wall.

Recent numerical codes are able to assess the role of several refurbishment techniques on masonry components [31,32] taking into account their dynamical performances near collapse.

In the last few years, the insertion of Fiber Reinforced Polymers (FRP) has been common, mainly with Carbon (CFRP) or Glass (GFRP). FRP are helpful in reducing the impact of the above techniques [33,34]. FRP are used for external surface reinforcements [35] or to create internal frames inside the masonry system [36]. The use of polymers to strengthen masonry subjected to blast loads has been reviewed in [37] with an experimental data set collected from several papers. A special mention is deserved by [38], which refers to the application of a sprayed-on polymer on masonry walls.

Analysis of several types of interventions, in terms of cost-benefits, is in [39] on a set of buildings in the Lisbon area with several fragility curves. A recent approach to join structural retrofitting with energy properties is presented in [40], where the problem of associating a cost-benefit to each different retrofitting procedure is compared with alternative choices in order to optimize the refurbishments.

2.2. Energy Retrofitting

A review of the state-of-the-art energy retrofitting methods to existing buildings is in [41]. After it outlines methods to enhance the energy efficiency from previous studies, it summarizes the following actions:

- improvement of thermal performance of building façades,
- optimization of building insulation,
- modification of indoor temperature set-points,
- improvement of the heating system efficiency,
- installation of energy saving lighting and air ventilation control.

An example of these approaches is in [42], where an historical masonry building in Benevento (Italy) is analyzed. Six retrofitting actions are modelled: modification of the indoor temperatures, reduction of the air draught, increase of the vertical wall thermal insulation, replacement of the boiler with a condensation gas heater, and substitution of the windows. It yields a reduction of the primary energy demand of more than 20%. An important trend is the multi-criteria optimization of the energy performance of buildings. In [43], it is applied to the renovation strategy of some historical masonry buildings in Algeria. In [44] a comparative analysis among different on-site construction systems and materials (wood, steel, and concrete) is presented. It is of interest to compare the energy consumed in the construction process with respect to the total initial embodied energy and greenhouse gas emissions.

Special attention has been devoted to the improvement of thermal insulation and waterproofing properties of masonry walls. A detailed description of the main thermal insulation techniques is in [45,46]. The current systems to build masonry walls with high thermal insulation properties are described in [47]. The technique of Light Weight Concrete (LWC) blocks for thermal insulation is assessed with different arrangements of internal holes or components of the mix design. Recently, the effect of alkaline activation in Compressed Earth Block (CEB) has been studied in [48]. It demonstrates how to reduce the heat transfer coefficient of a wall made of CEB. In [49,50] the effect of titanium dioxide and zinc oxide nano-particulate aqueous façade emulsions on brick walls was tested for water repellent and thermal insulation applications. The results show how this approach can reduce the energy consumption with an important financial saving. The advantageous use of blocks made of hemp fibers or cork grains with NHL (Natural Hydraulic Lime) is another option to improve sustainability by reducing extraction and production energies [51].

A significant application of masonry thermal insulation is reported in [52] where the performance of a refractory masonry glassmaking furnace is studied with a mathematical model. The main thermal insulation is provided by some rigid fiber boards and microporous sandwich boards with positive savings on furnace fuels. In [53], the efficiency of new coatings (realized with silica nano-particles and micro-clay enrichment of alkosiloxane) for brick waterproofing is assessed. In [54,55], different renovation strategies for existing building stock located in Sweden are outlined, depending on each climate zone, in order to furnish parameters for their optimization. Also, an Italian example [56] of analysis of cost-optimal performances shows the possibility to address the design in terms of energy efficiency.

2.3. Combined Seismic and Energy Retrofitting

A large number of papers deal with specific structural or energy retrofitting methods for masonry constructions. Although few researchers have worked on an integrated approach capable of taking into account both issues. A recent paper by Triantafillou et al. [57] discusses the structural and energy performance of a new retrofitting system based on TRM and thermal insulating materials. Medium scale experimental tests were performed on 17 masonry walls subjected to out of plane bending; the combination of TRM jacketing and thermal and fire-resistant insulation proved to be effective. In addition, energy based approaches were recently implemented to assess structural performances in [58], which made a possibly profitable suggestion to use energy as a synthetic parameter to evaluate the vulnerability of a masonry component.

The previously mentioned contribution by Calvi et al. [9] introduces the Green and Resilient Indicator (GRI), after the definition of specialized indicators, the energy expected annual loss, EAL_E, is:

$$EAL_E = \frac{mean\ annual\ energy\ cost}{total\ building\ value}, \tag{1}$$

While the seismic expected annual loss, EAL_s, is:

$$EAL_s = \frac{expected\ annual\ seismic\ lost}{total\ building\ value}. \tag{2}$$

The annual energy cost is easily calculated from the contributions necessary for the thermal comfort of the building given its location and its thermal characteristics. On the other hand, the expected annual seismic loss is evaluated considering the standard seismic load of its location and its structural characteristics. An example to evaluate seismic damage costs are in [59]. From an energy point of view, the evaluation of the thermal resistance of the building (reciprocal of the thermal transmittance) joined with the thermal performance requested by technical standards, can furnish the corresponding costs. From a structural point of view, a push-over analysis can assess the inter-story drift linked to seismic damage evaluation and performance levels by structural codes or documents (see [60,61]). Then, given the damages, it is easy to calculate the cost of the needed refurbishments. The indicators EAL_E and $EALs$ are cumulative components of the GRI definition and allow for the comparison of several retrofitting strategies. three case studies are in [9], with different reinforced concrete building types characterized by different functions and locations.

3. An Example of an Integrated Approach on Structural and Energy Features

For the sake of simplicity, the focus of this paper is limited to single masonry walls, although the proposed method can be extended to the entire building. With the aim of quantifying the effects of a retrofitting strategy, thermal and structural performances are considered. For each wall panel, it is possible to calculate the relative increment of structural resistance ΔR (in plane or out of plane) and the relative increment in the thermal resistance ΔU (reciprocal of the transmittance) obtained after an assigned retrofitting technique. Thus, they are:

$$\Delta R = (R_1 - R_0)/R_0, \tag{3}$$

$$\Delta U = (U_1 - U_0)/U_0. \tag{4}$$

where R_0 and U_0 are structural and thermal parameters before refurbishment, while R_1 and U_1 are after refurbishment. Both properties should be referred to at the specific site in which the building is erected. Considering as an example the Italian peninsula, the seismic events, commonly measured throughout the peak ground acceleration (PGA), are mapped in Figure 4. In the meanwhile, the thermal effect, commonly measured throughout the Degree Day (DD), is depicted in Figure 5. Thus, both aspects can be measured by the following dimensionless parameters $\boldsymbol{c_R}$ and $\boldsymbol{c_U}$

$$\boldsymbol{c_R} = \frac{PGA_i}{PGA_{MAX}}. \tag{5}$$

$$\boldsymbol{c_U} = \frac{DD_i}{DD_{MAX}}. \tag{6}$$

where PGA_{MAX} represents the maximum peak ground acceleration of the Italian peninsula and PGA_i is the peak ground acceleration for the considered i-th location of the building. In the same way, DD_{MAX} is the maximum Degree Day value for the same area and DD_i is the corresponding value for the given i-th location.

$\boldsymbol{c_R}$ and $\boldsymbol{c_U}$ parameters are a sort of "weight" of the structural and energy requirements in an assigned area. In the mentioned example, Italy is divided into 107 districts, assigning conventionally to each of them the values of PGA_i and DD_i of the main district town. The ratios in Equations (5) and (6) are determined to rank each district for both phenomena.

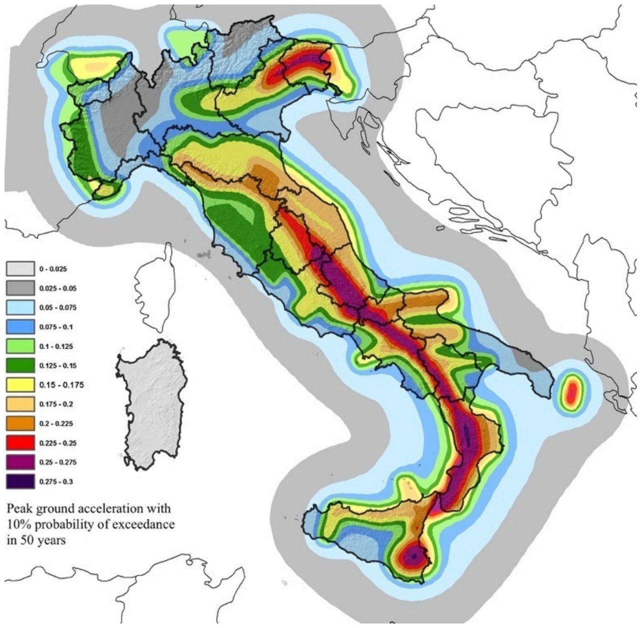

Figure 4. Italian map of seismic *PGA* (peak ground acceleration), taken from [62].

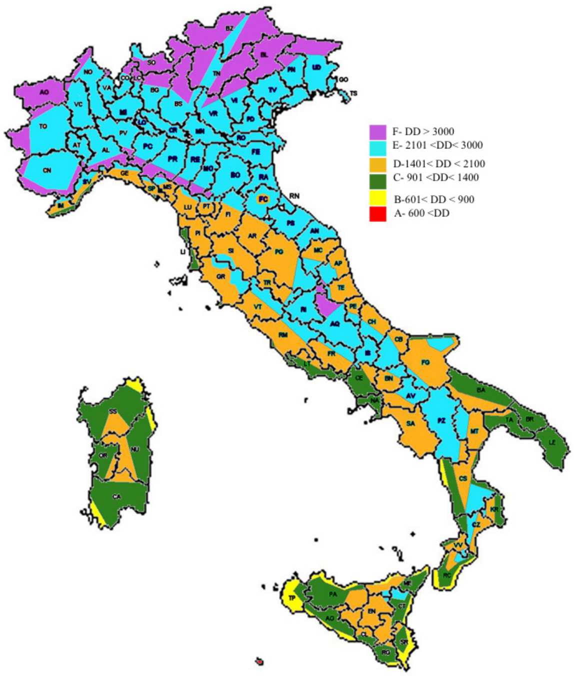

Figure 5. Italian map of heating *DD* (Degree Day), based on Italian technical code [63].

Let us first consider a loadbearing masonry wall of thickness t_m and length b_m, characterized by mechanical parameters f_m (compression strength), t_0 (shear strength), and a thermal parameter $1/\lambda_m$ (thermal resistance). To show the proposed method, it is assumed a building is located in two different emblematic sites in Italy: the first characterized by a low value of *PGA* and a high value of *DD* (i.e., Torino, Italy), the second (i.e., Catania, Italy) by a high value of *PGA* and a low value of *DD*. It also assumes, for the sake of simplicity, that the limit values of the axial force N_0 and of the shear force V_0 are proportional to the section area A_m of the wall:

$$N_0 = f_m\, A_m;\; V_0 = t_o\, A_m \tag{7}$$

The corresponding thermal resistance is

$$U_{c0} = (1/\lambda_X)\ A_m \tag{8}$$

Then, the following set of four possible refurbishment techniques (Figure 6) are examined:

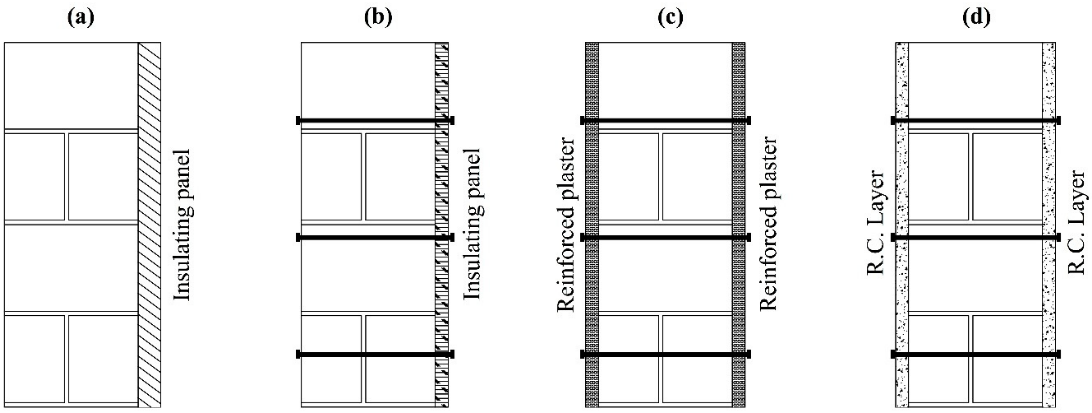

Figure 6. Proposed refurbishment techniques for masonry walls. (**a**) Single insulating panel by natural first choice cork and traditional plaster on both faces; (**b**) single polystyrene panel, transverse connectors and traditional plaster on both faces; (**c**) coupled GFRP (Glass Fiber Reinforced Polymer) plaster and transverse connectors; (**d**) coupled reinforced concrete layer and transverse connectors.

The four intervention techniques are emblematic. Intervention (a) does not appreciably increase the strength, while it enhances the thermal resistance to a new value of U_{A1}. Intervention (b) is aimed to increase the thermal resistance to U_{B1}, but is also able to induce a superior strength of R_{B1}. Intervention (c) is aimed to increase the strength to R_{C1}, but is also able to induce a superior thermal resistance of U_{C1}. Intervention (d) does not appreciably increase the thermal resistance due to the high transmittance of the concrete, while it enhances the strength to a new value R_{D1}.

The scope of the analysis is to individuate the best choice of refurbishment for the two locations: the first site (Torino, low *PGA* or c_R, high *DD* or c_U) will require more thermal improvements with respect to structural enforcement in comparison with those of the second site (Catania, high *PGA* or c_R, low *DD* or c_U). If "performance parameter" *P* is considered the investment cost of refurbishment C_i with respect to the total cost of the building C_{tot}, to compare the several refurbishments, the parameter P can be defined as

$$P = \frac{Ci}{C_{tot}} \tag{9}$$

To compare the effects of each refurbishment with the same *P*, the following rule is assumed:

$$(c_R\Delta\mathbf{R})^{\alpha} + (c_U\Delta\mathbf{U})^{\alpha} = P \tag{10}$$

where α is an adaptive coefficient. The following example explains the calculation method of α.

To calculate a numerical result, it is assumed there is a masonry wall of limestone bricks with a thickness of 40 cm. In case (a), simple natural cork 4.0 cm thick (λ = 0.05 W/mK thermal conductibility) is applied on the external side of the wall, improving the thermal resistance with a negligible contribution to structural resistance. In case (b), a polypropylene panel 3.6 cm thick (λ = 0.06 W/mK thermal conductibility) is applied with the insertion of structural transverse connectors; it allows an improvement of 50% to the equivalent mechanical characteristics of the masonry f_m, as in Italian code [64] (Appendix A table C8A 2.1.). In case (c), two layers (1.3 cm thick) of premixed lightweight plaster (λ = 0.08 W/mK thermal conductibility) reinforced by a GFRP net are applied. The improvement in the structural performance of the wall is calculated by homogenization of its cross section A_p. Given

E_p = 1.3 GPa, the plaster Young modulus, and E_m = 1.4 GPa, the corresponding masonry modulus, the homogenized cross section A_i is:

$$A_i = A_m + A_p \times E_p/E_m. \tag{11}$$

Finally, the case (d) presents a structural improvement with two layers of concrete, 20 mm thick, transversally connected to the sides of the wall by steel connectors and reinforced by a micro-steel net. The compressive strength of concrete is f_{ck} = 25 MPa, while its thermal resistance improvement is negligible. The four described techniques are calibrated to have the same investment cost.

The first site is Torino (Italy) with a reference *PGA* value of 0.055 g and a *DD* value of 2617. In the Italian peninsula, the maximum values are in Aosta for *DD* (2850) and Reggio Calabria for *PGA* (0.270). Thus, we can obtain c_R = 0.055/0.270 = 0.767; c_U = 2617/2850 = 0.918. The second site is Catania (Italy) with a reference *PGA* value of 0.207 g and a *DD* value of 833. Compared to the same Italian area, we can obtain c_R = 0.207/0.270 = 0.767; c_U = 833/2850 = 0.292.

The improvements in structural and energy properties were calculated for the four cases and the corresponding points are reported in the diagram of Figure 7. Considering each point belonging to a similar iso-performance curve *P* = cost, it is then possible to perform a squared interpolation (α = 2.00) for the Catania site (red line in Figure 7) and the Torino site (blue line in Figure 7).

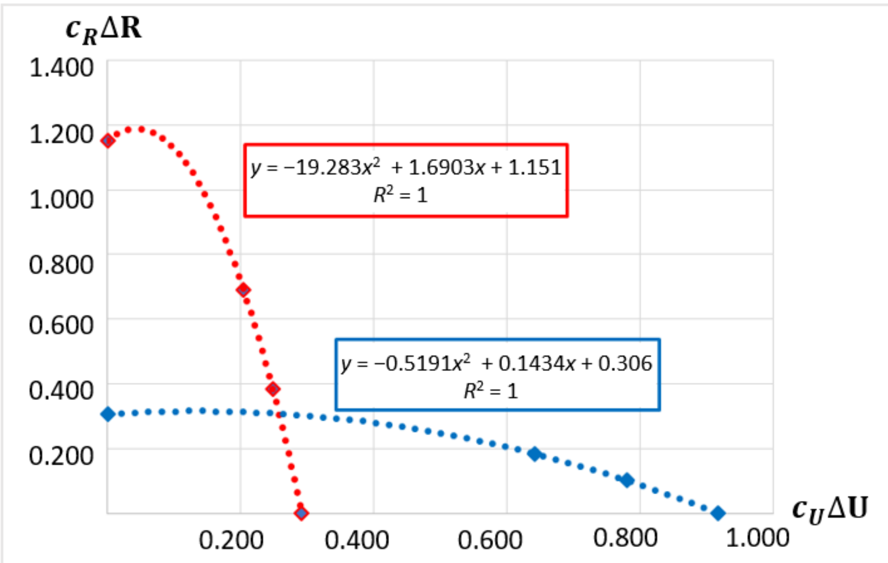

Figure 7. ($c_U\Delta$U, $c_R\Delta$R) diagrams (red: Catania; blue: Torino) interpolating the four techniques.

The performance parameter *P* identifies the cost of intervention; increasing *P* increases the budget for refurbishment. It is also possible to plot a series of curves, for each site, with different values of *P*. Moreover, the intersection of the two curves in Figure 7 identifies the intervention that would generate the same performance in both sites. Finally, each curve permits a comparison of the effects of each technique in the same location with equal investment cost.

4. A Generalized Combined Approach of Structural and Energy Aspects

The Index of seismic risk is typically related to three parameters: *structural vulnerability* (quality of the building), *seismic hazard of the location* (quality of the site), and *exposure of the destination* (relevance of use) [40]. Also, the thermal performance of a construction can be related to a set of three similar parameters: *thermal conductivity* (quality of the building), *thermal characteristics of the location* (quality of the site), and *exposure of the destination* (relevance of use). Thus, the performance parameter *P* of a wall, related to both aspects (structural and thermal) can be defined as the sum of two products of three components. *P* can measure the investment cost, but also the maintenance cost or other significant aspects. Considering the location of the buildings, its structural and thermal properties, and its level of importance, the value of two combination coefficients can be assessed with a single dimensionless performance parameter P by:

$$g_R(c_R\Delta\mathbf{R})^{\alpha_R} + g_U(c_U\Delta\mathbf{U})^{\alpha_U} = P \tag{12}$$

where (g_R, α_R) and (g_U, α_U) are dimensionless adaptive coefficients, respectively, of the structural and thermal aspects determined from experimental data. The dimensionless terms (c_R, c_U) can be calculated considering the peak ground acceleration (*PGA*) and the weather characteristics (i.e., the Degree Day or *DD*) of the site as shown in formulas (5) and (6). The dimensionless parameters (g_R, g_U) represent the specific weights that can be assumed for the structural or thermal improvement, depending on the use of the building. In this way, it is possible to compare different retrofitting strategies considering the specific characteristic of each location and of each socio-economical condition (i.e., expected seismic safety, expected thermal comfort, or energy consumption). In this sense, the performance parameter P can represent the investment cost of a refurbishment technique, or the maintenance cost, or the environmental cost (i.e., consumption of CO_2), or a social cost (i.e., rate of involved population), to determine thorough management decisions. A series of curves with prescribed P in the plane ($\Delta\mathbf{R}$, $\Delta\mathbf{U}$) from equation (12) are qualitatively plotted in Figure 8.

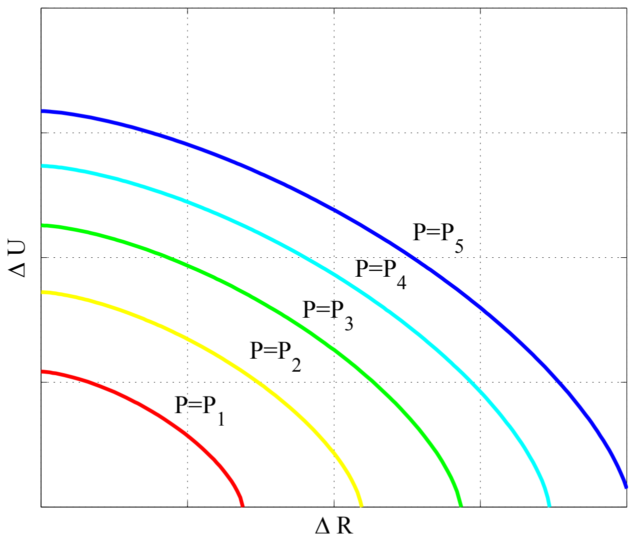

Figure 8. Qualitative curves for a given performance parameter P from equation (12).

A more detailed analysis can be done by introducing further quantities to describe the structural and thermal phenomena. It is possible to define another relevant structural parameter that measures the variation of the flexibility (reciprocal of stiffness) of the wall. It consists of the variation of the drift D of the wall (ratio between the transverse displacement and the height) that is strictly linked to the stiffness and flexibility characteristics of the structure. In the meanwhile, a further energy parameter can be adopted to measure the variation of the periodic transmittance, related to the variation of inertial mass M of the wall. Thus defining

$$\Delta \mathrm{D} = (\mathrm{D}_1 - \mathrm{D}_0)/\mathrm{D}_0, \tag{13}$$

$$\Delta \mathrm{M} = (\mathrm{M}_1 - \mathrm{M}_0)/\mathrm{M}_0, \tag{14}$$

it can obtain a more detailed performance parameter P as:

$$g_R(c_R\Delta\mathbf{R})^{\alpha_R} + g_D(c_D\Delta\mathbf{D})^{\alpha_D} + g_U(\mathrm{c}_U\Delta\mathbf{U})^{\alpha_\mathrm{U}} + g_M(\mathrm{c}_M\Delta\mathbf{M})^{\alpha_\mathrm{M}} = P \tag{15}$$

Also, in the last formula, the dimensionless adaptive coefficients (g_i, α_i) can give a different "weight" to each structural or energy property that contributes to *P*.

As previously mentioned, it is possible to consider one of the following set of performance parameters to compare each of the above techniques "before and after" refurbishment:

1. investment cost
2. maintenance cost
3. environmental cost (i.e., consumption of CO_2)
4. social cost (i.e., rate of involved population).

The explained example in Section 3 is based on the first parameter. In fact, it is also possible to change the meaning of the performance parameter *P*. For example, it can represent the maintenance cost, the environmental cost, or a social cost, and consequently, in order to obtain the iso-performance curves presented in Figure 7 or Figure 8, it is necessary to calibrate the four refurbishment techniques to achieve the same performance parameter *P*.

5. Conclusions and Perspectives

The constructive management of existing constructions should take into account both the structural safety, the energy cost, and the comfort conditions of the building. In particular, in the case of masonry buildings, structural retrofitting can be matched by the energy cost in the set of possible renovation strategies. The cost-benefit analysis necessary to find the optimum solution needs synthetic performance indicators which, as yet, have not been investigated. Indeed, only a few studies have been developed on integrated solutions based on both structural and energy needs of existing structures. In this work, a brief review of state-of-the-art structural and energy retrofitting techniques for existing masonry buildings was reported. Then, the definition of a new synthetic performance parameter *P* was presented through an example and a more generalized approach. This new parameter is capable of representing the retrofitting improvement in structural safety and in thermal insulation for each masonry wall.

Further developments of this research are expected with the application to several case studies necessary to determine the best values for the adaptive coefficients (α_i). It would be interesting to enhance the method giving a better definition of the "comfort" inside the building, for example, considering also the hygrometric and acoustic conditions, etc. Finally, an extension of this approach for the complete construction is sought with the aim of obtaining diagrams like the ones presented in Figures 7 and 8 that can be useful for the early design of retrofitting for existing buildings.

Acknowledgments: The financial support of ReLUIS-DPC2017—PR1 (Masonry) is acknowledged.

Author Contributions: Mauro Sassu conceived the illustrated strategy and the theoretical formulation; Flavio Stochino analyzed the numerical results and contributed to the theoretical formulation; Fausto Mistretta provided the refurbishment solutions. All the authors wrote the paper.

Conflicts of Interest: The authors declare no conflict of interest.

References

1. Stochino, F.; Mistretta, F.; Meloni, P.; Carcangiu, G. Integrated approach for post-fire reinforced concrete structures assessment. *Period. Polytech. Civ.* **2017**. [CrossRef]
2. Acito, M.; Stochino, F.; Tattoni, S. Structural response and reliability analysis of RC beam subjected to explosive loading. *AMM* **2011**, *82*, 434–439. [CrossRef]
3. Stochino, F. RC beams under blast load: Reliability and sensitivity analysis. *Eng. Fail. Anal.* **2016**, *66*, 544–565. [CrossRef]
4. Giovino, G.; Olmati, P.; Garbati, S.; Bontempi, F. Blast resistance assessment of concrete wall panels: Experimental and numerical investigations. *Int. J. Prot. Struct.* **2014**, *5*, 349–366. [CrossRef]
5. Sassu, M. The Reinforced Cut Wall (RCW): A Low-Cost Base Dissipator for Masonry Buildings. *Earthq. Spectra* **2016**, *22*, 533–554. [CrossRef]

6. Sassu, M. Biaxiality effect on the energy dissipated by elastoplastic base-isolators. *J. Eng. Mech. ASCE* **2003**, *22*, 533–554. [CrossRef]
7. Asteris, P.G.; Chronopoulos, M.P.; Chrysostomou, C.Z.; Varum, H.; Plevris, V.; Kyriakides, N.; Silva, V. Seismic vulnerability assessment of historical masonry structural systems. *Eng. Struct.* **2014**, *62*, 118–134. [CrossRef]
8. Tesfamariam, S.; Sadiq, R.; Najjaran, H. Decision making under uncertainty—An example for seismic risk management. *Risk Anal.* **2010**, *30*, 78–94. [CrossRef] [PubMed]
9. Calvi, G.M.; Sousa, L.; Ruggeri, C. Energy Efficiency and Seismic Resilience: A Common Approach. In *Multi-Hazard Approaches to Civil Infrastructure Engineering*; Gardoni, P., La Fave, J.M., Eds.; Springer International Publishing: Basel, Switzerland, 2016; pp. 165–208.
10. El Gawady, M.; Lestuzzi, P.; Badoux, M. A review of conventional seismic retrofitting techniques for URM. In Proceedings of the 13th International Brick and Block Masonry Conference, Amsterdam, The Netherlands, 4–7 July 2004; pp. 1–10.
11. Montes, P.; Fernandez, A. Behaviour of a hemispherical dome subjected to wind loading. *J. Wind Eng. Ind. Aerodyn.* **2001**, *89*, 911–924. [CrossRef]
12. Jabarov, M.; Kozharinov, S.; Lunyov, A. Strengthening of damaged masonry by reinforced mortar layers. In Proceedings of the 7th WCEE, Istanbul, Turkey, 8–13 September 1980; Volume 6, pp. 73–80.
13. Tomazevic, M. *Earthquake-Resistant Design of Masonry Buildings*; World Scientific: Singapore, 1999; Volume 1.
14. Karantoni, F.V.; Fardis, M.N. Effectiveness of seismic strengthening techniques for masonry buildings. *J. Struct. Eng. ASCE* **1992**, *118*, 1884–1902. [CrossRef]
15. Kahn, L. Shotcrete retrofit for unreinforced brick masonry. In Proceedings of the 8th WCEE, San Francisco, CA, USA, 21–28 July 1984; pp. 583–590.
16. Prota, A.; Marcari, G.; Fabbrocino, G.; Manfredi, G.; Aldea, C. Experimental in plane behaviour of tuff masonry strengthened with cementitious matrix-grid composites. *J. Compos. Constr.* **2006**, *10*, 223–233. [CrossRef]
17. Papanicolaou, C.G.; Triantafillou, T.C.; Karlos, K.; Papathanasiou, M. Textile reinforced mortar (TRM) versus FRP as strengthening material of URM walls: In-Plane cyclic loading. *Mater. Struct.* **2007**, *40*, 1081–1097. [CrossRef]
18. Papanicolaou, C.G.; Triantafillou, T.C.; Papathanasiou, M.; Karlos, K. Textile reinforced mortar (TRM) versus FRP as strengthening material of URM walls: Out-of-Plane cyclic loading. *Mater Struct.* **2008**, *41*, 143–157. [CrossRef]
19. Parisi, F.; Lignola, G.P.; Augenti, N.; Prota, A.; Manfredi, G. Nonlinear behaviour of a masonry subassemblage before and after strengthening with inorganic matrix-grid composites. *J. Compos. Constr.* **2011**, *15*, 821–832. [CrossRef]
20. Babaeidarabad, S.; De Caso, F.; Nanni, A. Out-of-plane behavior of URM walls strengthened with fabric-reinforced cementitious matrix composite. *J. Compos. Constr.* **2014**, *18*, 04013057. [CrossRef]
21. Calvi, G.; Magenes, G. Experimental results on unreinforced masonry shear walls damaged and repaired. In Proceedings of the 10th IB2MaC, Calgary, AB, Canada, 5–7 July 1994; pp. 509–518.
22. Schuller, M.; Atkinson, R.; Borgsmiller, J. Injection grouting for repair and retrofit of unreinforced masonry. In Proceedings of the 10th IB2MaC, Calgary, AB, Canada, 5–7 July 1994; pp. 549–558B.
23. Papanicolaou, C.; Triantafillou, T.; Lekka, M. Externally bonded grids as strengthening and seismic retrofitting materials of masonry panels. *Constr. Build Mater.* **2011**, *25*, 504–514. [CrossRef]
24. Borri, A.; Corradi, M.; Speranzini, E.; Giannantoni, A. Consolidation and Reinforcing of stone wall using a reinforced repointing grid. In Proceedings of the 6th International Conference of Structural Analysis of Historical Construction, Bath, UK, 2–4 July 2008.
25. Giresini, L.; Sassu, M. Horizontally restrained rocking blocks: Evaluation of the role of boundary conditions with static and dynamic approaches. *Bull. Earthq. Eng.* **2017**, *15*, 385–410. [CrossRef]
26. Giresini, L.; Fragiacomo, M.; Sassu, M. Rocking analysis of masonry walls interacting with roofs. *Eng. Struct.* **2016**, *116*, 107–120. [CrossRef]
27. Yu, Z.; Zhengyun, W.; Weiping, Z. Experimental research on aseismic strengthening of block masonry buildings using thin structural columns. In Proceedings of the 11th IB2MaC, Shanghai, China, 14–16 October 1997; pp. 626–633.

28. Chuxian, S.; Guiqiu, L.; Wenchao, W. The design of Brick masonry structure with concrete column. In Proceedings of the 11th IB2MaC, Shanghai, China, 14–16 October 1997; pp. 626–633.
29. Lissel, S.; Shrive, N. Construction of diaphragm walls post-tensioned with carbon fiber reinforced polymer tendons. In Proceedings of the 9th NAMC, Clemson, SC, USA, 9 June 2003; pp. 192–203.
30. Rosenboom, O.; Kowalsky, M. Investigation of alternative details for seismic design of post-tensioned clay masonry walls. In Proceedings of the 9th NAMC, Clemson, SC, USA, 9 June 2003; pp. 475–485.
31. Casapulla, C.; Cascini, L.; Portioli, F.; Landolfo, R. 3D macro and micro-block models for limit analysis of out-of-plane loaded masonry walls with non-associative Coulomb friction. *Meccanica* **2014**, *49*, 1653–1678. [CrossRef]
32. Casapulla, C.; Jossa, P.; Maione, A. Rocking motion of a masonry rigid block under seismic actions: A new strategy based on the progressive correction of the resonance response. *Ing. Sismica* **2010**, *27*, 35–48.
33. Ehsani, M.R.; Saadatmanesh, H.; Al-Saidy, A. Shear behavior of URM retrofitted with FRP overlays. *J. Compos. Constr.* **1997**, *1*, 17–25. [CrossRef]
34. Albert, M.L.; Elwi, A.E.; Cheng, J.R. Strengthening of unreinforced masonry walls using FRPs. *J. Compos. Constr.* **2001**, *5*, 76–84. [CrossRef]
35. Gattesco, N.; Boem, I.; Dudine, A. Diagonal compression tests on masonry walls strengthened with a GFRP mesh reinforced mortar coating. *Bull. Earthq. Eng.* **2015**, *13*, 1703–1726. [CrossRef]
36. Priestley, M.J.N.; Seible, F. Design of seismic retrofit measures for concrete and masonry structures. *Constr. Build. Mater.* **1995**, *9*, 365–377. [CrossRef]
37. Buchan, P.A.; Chen, J.F. Blast resistance of FRP composites and polymer strengthened concrete and masonry structures—A state-of-the-art review. *Compos. Eng. Part B* **2007**, *38*, 509–522. [CrossRef]
38. Davidson, J.S.; Porter, J.R.; Dinan, R.J.; Hammons, M.I.; Connell, J.D. Explosive testing of polymer retrofit masonry walls. *J. Perform. Constr. Facil.* **2004**, *18*, 100–106. [CrossRef]
39. Marques, R.; Lamego, P.; Lourenco, P.B.; Sousa, M.L. Efficiency and cost-benefit analysis of seismic strengthening techniques for old residential buildings in Lisbon. *J. Earthq. Eng.* **2017**, 1–36. [CrossRef]
40. Calvi, G.M. Choices and criteria for seismic strengthening. *J. Earthq. Eng.* **2013**, *17*, 769–802. [CrossRef]
41. Ma, Z.; Cooper, P.; Daly, D.; Ledo, L. Existing building retrofits: Methodology and state-of-the-art. *Energy Build.* **2012**, *55*, 889–902. [CrossRef]
42. Ascione, F.; De Rossi, F.; Vanoli, G.P. Energy retrofit of historical buildings: Theoretical and experimental investigations for the modelling of reliable performance scenarios. *Energy Build.* **2011**, *43*, 1925–1936. [CrossRef]
43. Seddiki, M.; Anouche, K.; Bennadji, A.; Boateng, P. A multi-criteria group decision-making method for the thermal renovation of masonry buildings: The case of Algeria. *Energy Build.* **2016**, *129*, 471–483. [CrossRef]
44. Cole, R.J. Energy and greenhouse gas emissions associated with the construction of alternative structural systems. *Build. Environ.* **1998**, *34*, 335–348. [CrossRef]
45. Al-Homoud, M.S. Performance characteristics and practical applications of common building thermal insulation materials. *Build. Environ.* **2005**, *40*, 353–366. [CrossRef]
46. Jelle, B.P. Traditional, state-of-the-art and future thermal building insulation materials and solutions—Properties, requirements and possibilities. *Energy Build.* **2011**, *43*, 2549–2563. [CrossRef]
47. Al-Jabri, K.S.; Hago, A.W.; Al-Nuaimi, A.S.; Al-Saidy, A.H. Concrete blocks for thermal insulation in hot climate. *Cem. Concr. Res.* **2005**, *35*, 1472–1479. [CrossRef]
48. Leitão, D.; Barbosa, J.; Soares, E.; Miranda, T.; Cristelo, N.; Briga-Sá, A. Thermal performance assessment of masonry made of ICEB's stabilised with alkali-activated fly ash. *Energy Build.* **2017**, *139*, 44–52. [CrossRef]
49. Mac Mullen, J.; Zhang, Z.; Radulovic, J.; Herodotou, C.; Totomis, M.; Dhakal, H.N.; Bennett, N. Titanium dioxide and zinc oxide nano-particulate enhanced oil-in-water (O/W) facade emulsions for improved masonry thermal insulation and protection. *Energy Build.* **2012**, *52*, 86–92. [CrossRef]
50. Zhang, Z.; Mac Mullen, J.; Dhakal, H.N.; Radulovic, J.; Herodotou, C.; Totomis, M.; Bennett, N. Enhanced water repellence and thermal insulation of masonry by zinc oxide treatment. *Energy Build.* **2012**, *54*, 40–46. [CrossRef]
51. Sassu, M.; Giresini, L.; Bonannini, E.; Puppio, M.L. On the Use of Vibro-Compressed Units with Bio-Natural Aggregate. *Buildings* **2016**, *6*, 40. [CrossRef]
52. Dzyuzer, V.Y.; Shvydkii, V.S. Thermal Insulation of the Refractory Masonry in Glassmaking Furnaces. *Glass Ceram.* **2015**, *71*, 365–368. [CrossRef]

53. Stefanidou, M.; Karozou, A. Testing the effectiveness of protective coatings on traditional bricks. *Constr. Build. Mater.* **2016**, *111*, 482–487. [CrossRef]
54. Mata, E.; Sasic Kalagasidis, A.; Johnsson, F. Cost-effective retrofitting of Swedish residential buildings: Effects of energy price developments and discount rates. *Energy Effic.* **2015**, *8*, 223–237. [CrossRef]
55. Tronchin, L.; Tommasino, M.C.; Fabberi, K. On the cost-optimal levels of energy-performance requirements for buildings: A case study with economic evaluation in Italy. *Int. J. Sustain. Energy Plan. Manag.* **2014**, *3*, 49–62.
56. Bonakdar, F.; Kalagasidis, A.S.; Mahapatra, K. The Implications of Climate Zones on the Cost-Optimal Level and Cost-Effectiveness of Building Envelope Energy Renovation and Space Heat Demand Reduction. *Buildings* **2017**, *7*, 39. [CrossRef]
57. Triantafillou, T.C.; Karlos, K.; Kefalou, K.; Argyropoulou, E. An innovative structural and energy retrofitting system for URM walls using textile reinforced mortars combined with thermal insulation: Mechanical and fire behavior. *Constr. Build. Mater.* **2017**, *133*, 1–13. [CrossRef]
58. Giresini, L. Energy-based method for identifying vulnerable macro-elements in historic masonry churches. *Bull. Earthq. Eng.* **2016**, *14*, 919–942. [CrossRef]
59. Lamego, P.; Lourenço, P.B.; Sousa, M.L.; Marques, R. Seismic vulnerability and risk analysis of the old building stock at urban scale: Application to a neighbourhood in Lisbon. *Bull. Earthq. Eng.* **2017**, *15*, 2901–2937. [CrossRef]
60. Federal Emergency Management Agency. *Prestandard and Commentary for the Seismic Rehabilitation of Buildings (FEMA Publication No. 356)*; the American Society of Civil Engineers for the Federal Emergency Management Agency: Washington, DC, USA, 2000.
61. Structural Engineers Association of California. *Vision 2000—A Framework for Performance-Based Engineering*; Structural Engineers Association of California: Sacramento, CA, USA, 1995.
62. Italian Institute of Geophysics and Volcanology: Map of seismic hazard. Available online: https.www.ingv.it (accessed on 1 June 2017).
63. Italian Technical Norm on Energy Regulations. Available online: http://www.gazzettaufficiale.it/eli/id/1993/10/14/093G0451/sg (accessed on 1 June 2017).
64. Circ.2009-Instructions for "Technical Norms for Constructions". Available online: http://cslp.mit.gov.it/index.php?option=com_content&task=view&id=79&Itemid=20 (accessed on 1 June 2017).